

**Band-structure calculations for the 3d transition metal oxides in GW**

Stephan Lany

*National Renewable Energy Laboratory, Golden, Colorado 80401, USA*

(Received 3 October 2012; revised manuscript received 23 January 2013; published 13 February 2013)

Many-body *GW* calculations have emerged as a standard for the prediction of band gaps, band structures, and optical properties for main-group semiconductors and insulators, but it is not well established how predictive the *GW* method is in general for transition metal (TM) compounds. Surveying the series of 3d oxides within a typical *GW* approach using the random-phase approximation reveals mixed results, including cases where the calculated band gap is either too small or too large, depending on the oxidation states of the TM (e.g., FeO/Fe<sub>2</sub>O<sub>3</sub>, Cu<sub>2</sub>O/CuO). The problem appears to originate mostly from a too high average *d*-orbital energy, whereas the splitting between occupied and unoccupied *d* symmetries seems to be reasonably accurate. It is shown that augmenting the *GW* self-energy by an attractive (negative) and occupation-independent on-site potential for the TM *d* orbitals with a single parameter per TM cation can reconcile the band gaps for different oxide stoichiometries and TM oxidation states. In Cu<sub>2</sub>O, which is considered here in more detail, standard *GW* based on wave functions from initial density or hybrid functional calculations yields an unphysical prediction with an incorrect ordering of the conduction bands, even when the magnitude of the band gap is in apparent agreement with experiment. The correct band ordering is restored either by applying the *d*-state potential or by iterating the wave functions to self-consistency, which both have the effect of lowering the Cu-*d* orbital energy. While it remains to be determined which improvements over standard *GW* implementations are needed to achieve an accurate *ab initio* description for a wide range of transition metal compounds, the application of the empirical on-site potential serves to mitigate the problems specifically related to *d* states in *GW* calculations.

DOI: [10.1103/PhysRevB.87.085112](https://doi.org/10.1103/PhysRevB.87.085112)

PACS number(s): 71.15.-m, 71.27.+a, 78.20.-e, 88.40.fh

**I. INTRODUCTION**

The band-structure properties of semiconducting or insulating materials are essential for their functionality in a wide spectrum of electronic and optoelectronic applications, ranging from integrated circuits to light-emitting diodes and solar cells. Whereas conventional semiconductor technologies are mostly based on main-group compounds, emerging materials often contain transition metals; examples include TiO<sub>2</sub> as a transparent conducting oxide,<sup>1</sup> Fe chalcogenides<sup>2</sup> and Cu<sub>2</sub>O (Refs. 3,4) as photovoltaic solar absorbers, or Fe<sub>2</sub>O<sub>3</sub> as a photoelectrocatalyst.<sup>5</sup>

Many-body perturbation theory in the *GW* approximation<sup>6</sup> has emerged as the primary computational tool for the band-structure prediction of semiconductors and insulators,<sup>7–17</sup> providing a systematic improvement of band structures calculated in the local-density or generalized gradient approximations (LDA or GGA) to density functional theory (DFT). The past decade has seen considerable developments and discussions around a number of issues related to the *GW* method: concerning the technical implementation, such as pseudopotential vs all electron methods,<sup>16,18</sup> the issue of core-valence partitioning,<sup>12,16,19</sup> and pseudopotential scattering properties at high energies;<sup>20</sup> concerning convergence parameters, such as the number of unoccupied bands;<sup>21,22</sup> concerning approximations for the screened Coulomb interaction *W*, such as the plasmon pole model,<sup>22</sup> the random-phase approximation (RPA),<sup>14</sup> or vertex corrections and excitonic effects beyond RPA;<sup>13,23</sup> and concerning the degree of self-consistency of both the eigenenergies and the wave functions.<sup>9,11–14,24</sup>

While there is presently no single universally accepted scheme for *GW* calculations, a fairly consistent description of band gaps and band structures can be achieved for *main-group semiconductors and insulators*, where the following

picture is emerging: (i) A single iteration of a *GW* update (“*G<sub>0</sub>W<sub>0</sub>*”) of the single-particle energies is sufficient only if the quasiparticle energy (QPE) shifts are relatively small. Thus, one can either iterate the eigenenergies to self-consistency, or use a suitable density functional or hybrid functional so that the initial band energies are already close to the *GW* QPE.<sup>14,15,17</sup> (ii) The calculation of *W* in the RPA leads to a significant, but systematic overestimation of the band gaps, due to an underestimated screening.<sup>11,14</sup> Strategies to compensate this overestimation include a scaling of the QPE shifts,<sup>25</sup> maintaining the screened Coulomb interaction *W<sub>0</sub>* from the first iteration for subsequent *GW* iterations,<sup>14</sup> or including vertex corrections in the calculation of *W* interactions.<sup>13,23,26</sup> (iii) In systems with shallow 3d states such as the Zn-VI compounds, the 3d binding energy is underestimated by more than 1 eV.<sup>7,8,10,13,14</sup> However, the resulting effect on the band-edge states is usually rather small, except for the case of ZnO where the band gap is reduced by about 0.3 eV due to the stronger O-*p*/Zn-*d* interaction.<sup>27</sup> (iv) Comparing literature results from calculations with<sup>11,13</sup> and without<sup>14,15,17</sup> inclusion of the nondiagonal components of the *GW* self-energy, it appears that the self-consistency in the wave functions has a rather limited effect for main-group compounds.

Considering *transition metal compounds* and specifically transition metal oxides, the situation is much less clear. While *GW* calculations in various flavors have been reported, e.g., for Cu<sub>2</sub>O,<sup>24,28,29</sup> TiO<sub>2</sub>,<sup>30</sup> Fe<sub>2</sub>O<sub>3</sub>,<sup>31</sup> and several transition metal (TM) monoxides,<sup>9,32,33</sup> a comprehensive study of the complete 3d series of TM oxides within a single *GW* scheme is not available. However, surveying the present literature gives clear hints that the consistent description of TM compounds is difficult within a single approach: For example, the *G<sub>0</sub>W<sub>0</sub>*(HSE) approach (denoting a *G<sub>0</sub>W<sub>0</sub>* calculation based on initial calculation of wave functions and eigenvalues using

the HSE hybrid functional introduced in Ref. 34), that is considered to be reliable in main-group compounds<sup>15</sup> gives a much too large band gap of 4.0 eV in Fe<sub>2</sub>O<sub>3</sub>,<sup>31</sup> compared to the experimental gap at 2.1 eV.<sup>35</sup> The  $G_0W_0$ (LDA) variant, which underestimates the gap of ZnO by as much as 1 eV,<sup>7,22</sup> already overestimates the gap by 0.3 eV in TiO<sub>2</sub> (Ref. 30) and by 0.6 eV in SrTiO<sub>3</sub>.<sup>36</sup> The self-consistency in the wave functions was found to be essential for the correct band structure of Cu<sub>2</sub>O,<sup>24,28</sup> but in ZnO and GaN, the self-consistency did not correct the underbinding of the 3*d* states.<sup>13,37</sup> Thus, the purpose of the present study is to establish the trends along the 3*d* series of TM oxides in a single *GW* scheme.

## II. METHOD OF CALCULATION

The *GW* calculations in this work are performed within the projector augmented wave (PAW) (Refs. 38,39) implementation of the VASP code (version 5.2).<sup>19,39</sup> With the goal of a feasible scheme for high-throughput band-structure prediction in mind, computationally expedient PAW data sets were chosen for the present study: For oxygen, a “soft” potential was used, allowing for a relative small energy cutoff for the wave functions of 320 eV. This potential has been tested before, both in density functional and *GW* calculations.<sup>40,41</sup> For the early (Ti-Cr) and late (Mn-Cu) TM, the 3*p* shell was placed in the valence and in the core, respectively. Inclusion of the 3*s* shell in the valence for the early TM was found to lead only to marginal changes of the QPE of less than 0.1 eV. Inclusion of the 3*p* shell for the late TM had more significant effects up to a few tenths of an eV, but did not lead to a systematic improvement of band-gap energies compared to experiment.

The crystal and magnetic structures (NM = nonmagnetic, AF = antiferromagnetic, FI = ferrimagnetic), as well as the experimental data for band-gap energies have been obtained from a review of the following literature: TiO<sub>2</sub> (Ref. 42) (rutile, NM); V<sub>2</sub>O<sub>3</sub> (Refs. 43,44) (monoclinic, AF); VO<sub>2</sub> (Ref. 45) (distorted rutile, NM); V<sub>2</sub>O<sub>5</sub> (Refs. 46,47) (orthorhombic, NM); Cr<sub>2</sub>O<sub>3</sub> (Refs. 48–51) (corundum, AF); MnO (Refs. 52–54) (dRS = distorted rock salt, AF); Mn<sub>3</sub>O<sub>4</sub> (Refs. 55–57) (hausmannite, FI); FeO (Refs. 52,58) (dRS, AF); Fe<sub>2</sub>O<sub>3</sub> (Refs. 35,59,60) (corundum, AF); CoO (Refs. 52, 54,61) (dRS, AF); Co<sub>3</sub>O<sub>4</sub> (Refs. 62–64) (spinel, AF); NiO (Refs. 52,65–67) (dRS, AF); Cu<sub>2</sub>O (Refs. 68,69) (cuprite, NM); CuO (Refs. 70,71) (tenorite, AF). The crystal structures were relaxed in GGA + *U* (Refs. 72–74) with *U* = 5 eV for Cu and *U* = 3 eV for all other 3*d* TM. These values for *U* have recently been found to give a consistent description of the thermochemical properties,<sup>75</sup> and improve the description of the hybridization between the TM-*d* states with the O-*p* ligands, which is important when the wave functions of the initial DFT calculations are maintained during the *GW* calculation.<sup>27</sup> Furthermore, the treatment of correlation effects in DFT + *U* is necessary in many cases to restore the correct orbital symmetries and atomic structures, since LDA or GGA are often missing Jahn–Teller-like distortions in case of partially filled crystal field states of transition metal *d*-orbitals as present, e.g., in the orbital-ordered Mott insulator KCuF<sub>3</sub>.<sup>76</sup>

For the initial GGA + *U* calculation of eigenenergies and wave functions prior to the QPE calculations in *GW*, the cell volume was scaled to compensate for the typical overestima-

tion of the lattice constant by about 1% in GGA(+*U*). For the Brillouin-zone sampling, a  $\Gamma$ -centered *k*-mesh was used, where the number of subdivisions was taken such to obtain a total number of at least 1000/*n* *k*-points, where *n* is the number of atoms in the respective unit cell. The total number of bands was taken as 64 × *n*, leading to a convergence of the absolute QPE to about 0.1 eV. The energy cutoff for the response functions in *GW* was 150 eV. Spin-orbit interactions were not considered.<sup>77</sup> The HSE hybrid functional<sup>34</sup> has been used as an alternative Hamiltonian to generate the wave functions and initial eigenvalues.

## III. BAND GAPS OF 3*d* OXIDES IN BASELINE *GW* CALCULATIONS

As a baseline *GW* scheme, the screened Coulomb potential *W* is calculated in the random-phase approximation (RPA). While the GGA + *U* wave functions are fixed, the eigenenergies are iterated to self-consistency, to remove the strong dependence of the *GW* result on the initial DFT band-structure energies. Before comparing the calculated band gaps with experiment, however, it is worth noting that the available experimental data for transition metal oxides is often not as comprehensive and robust as for some main-group compounds (e.g., Si, GaAs, ZnO) where high-quality samples have been studied in great detail. The band-gap energies of TM oxides are usually determined either by optical measurements or by photoemission/inverse photoemission. Both types of data are not free of ambiguities: In principle, the (inverse) photoemission energies correspond to the QPE calculated by *GW*. However, photoemission probes mostly the energies with high density of states, e.g., originating from localized TM-*d* or O-*p* states, and are less sensitive to regions with small density of states, such as, e.g., the highly dispersive conduction bands occurring in many compound semiconductors. For example, the band gap of NiO, deduced from the band-edge structure measured by (inverse) photoemission, has been determined as 4.3 eV.<sup>66</sup> Optical absorption measurements, on the other hand, show an absorption threshold at only 3.5 eV,<sup>65,67</sup> and the difference could be due to a smaller density of states in the conduction band that might not be resolved in the inverse photoemission measurement. The optical characterizations are, however, also subject to uncertainties if the minimum band gap is indirect or optically forbidden, or when excitonic effects, including also internal *d-d* transitions, cause strong subgap absorption. Thus, a given absorption onset could signify the indirect/forbidden band gap (e.g., in a bulk sample), the direct-allowed band gap (e.g., in a thin film where phonon-assisted and disorder-induced transitions are too weak to contribute sufficiently to the absorption), the threshold for exciton generation (e.g., in wide-gap systems such as SiO<sub>2</sub> with large exciton binding energies<sup>20</sup>), or the excitation of internal *d-d* transitions [e.g., in Cr<sub>2</sub>O<sub>3</sub>, the absorption bands observed around 2.1 and 2.8 eV (Ref. 49) which coincide with well-known *d-d* internal excitations of octahedral Cr<sup>+III</sup>78]. These considerations need to be taken into account when interpreting optical measurements in terms of band-gap energies.

Table I shows the experimental band-gap energies from the literature in comparison with the results of the baseline  $GW^{\text{RPA}}$  calculations, and with calculations that include an

TABLE I. The band-gap energies for the series of  $3d$  oxides, comparing experimental literature data,  $GW$  in the random-phase approximation ( $GW^{\text{RPA}}$ ), and  $GW$  with local-field effects and empirical  $V_d$  potentials ( $GW^{\text{LF}} + V_d$ ). For the latter, also given are the direct (d) or indirect (i) nature of the gap, the absorption threshold energy  $E_{\text{abs}}$  for direct and allowed optical transitions (Ref. 84), the electronic static dielectric constant  $\epsilon$ , and the value of the parameter  $V_d$ .

	Expt. $E_g$ (eV)	$GW^{\text{RPA}}$ $E_g$ (eV)	$GW^{\text{LF}} + V_d$			
			$E_g$ (eV)	$E_{\text{abs}}$ (eV)	$\epsilon$	$V_d$ (eV)
TiO <sub>2</sub>	3.0	4.48	3.11 (i)	3.4	5.9	-1.1
V <sub>2</sub> O <sub>3</sub>	0.6	1.70	1.07 (i)	1.3	6.2	-2.8
VO <sub>2</sub>	0.6	1.12	0.46 (i)	0.9	9.5	
V <sub>2</sub> O <sub>5</sub>	2.3	4.69	1.85 (i)	2.4	4.9	
Cr <sub>2</sub> O <sub>3</sub>	3.2	4.75	3.23 (d)	3.3	5.9	-3.5
MnO	3.5	3.81	3.36 (i)	4.2	4.1	0
Mn <sub>3</sub> O <sub>4</sub>	2.5	2.89	2.49 (i)	2.5	4.7	
FeO	2.1	1.65	2.14 (i)	2.2	5.7	-2.0
Fe <sub>2</sub> O <sub>3</sub>	2.1	3.57	2.01 (i)	2.1	7.2	
CoO	2.8	3.23	2.80 (i)	3.3	5.3	-1.2
Co <sub>3</sub> O <sub>4</sub>	1.5	2.42	1.55 (d)	1.6	8.0	
NiO	3.5	4.28	3.48 (i)	3.7	6.5	-0.3
Cu <sub>2</sub> O	2.2	1.59 <sup>a</sup>	2.03 (d)	2.7	5.7	-2.4
CuO	1.6	2.49	1.19 (i)	1.4	7.9	

<sup>a</sup>Incorrect band ordering.

on-site potential for  $d$  states as discussed in Sec. IV below. While in main-group compounds, the RPA is known to lead to underestimated dielectric constants, and, hence, to overestimated band-gap energies ( $E_g$ ) (Refs. 11,14), it is apparent that  $GW^{\text{RPA}}$  gives mixed results in cases where the band gaps are much too large (e.g., TiO<sub>2</sub>, V<sub>2</sub>O<sub>5</sub>, Cr<sub>2</sub>O<sub>3</sub>, Fe<sub>2</sub>O<sub>3</sub>) and in cases where the band gaps are too small (FeO, Cu<sub>2</sub>O). As discussed in detail in Sec. V below, in case of Cu<sub>2</sub>O the discrepancy is much more dramatic than apparent from the band-gap energy, since the band ordering is wrong in  $GW^{\text{RPA}}$ . Note that similar trends and inconsistencies are also observed when using the HSE hybrid functional instead of GGA +  $U$  to calculate the initial eigenenergies and wave functions. The overall agreement with experiment is obviously much worse and less systematic than for similar types of calculations in main-group compounds,<sup>11–16</sup> suggesting that the discrepancies are associated with the presence of  $d$  states close to the band-edge energies.

At the present, the precise physical nature of difficulty to correctly describe the TM- $d$  states in  $GW$  is not entirely clear. While the imperfect description of the dielectric constant in RPA and incomplete self-interaction correction have been discussed as possible sources of the too high energies of occupied  $3d$  states in Zn-VI and Ga-V compounds,<sup>7,10,14</sup> these effects do not readily explain the too high energies of the unoccupied  $3d$  states that cause the too large band gaps in, e.g., TiO<sub>2</sub>, V<sub>2</sub>O<sub>5</sub>, and Fe<sub>2</sub>O<sub>3</sub> (see Table I). It also seems presently unclear which methodological improvements are needed for an accurate *ab initio*  $GW$  description of transition metal compounds. While the self-consistency in the wave functions significantly improves the band structure in Cu<sub>2</sub>O (Refs. 24,28; see also below), it does not correct the  $d$ -band position in ZnO.<sup>13,37</sup> Possible improvements may further result from excitonic effects (vertex corrections), or from improvements

of a more technical nature, such as the use of PAW potentials that have been specifically generated to yield better scattering properties at very high energies,<sup>20</sup> or the inclusion of more semicore states being explicitly treated as valence electrons. However, all of these options will increase the computational overhead considerably.

#### IV. $GW$ RESULTS WITH AN ON-SITE POTENTIAL TO ADJUST $d$ -ORBITAL ENERGIES

In the following, the objective is to find a workable  $GW$  scheme that allows for reasonably predictive band-structure calculation at an acceptable computational cost. As a first step to improve upon the RPA, the LDA derived local-field (LF) effects are included, which correspond to the adiabatic-LDA approximation within time-dependent DFT.<sup>79</sup> While these LF effects do not fully account for the electron-hole interaction, they lead to a somewhat increased dielectric constant  $\epsilon$ , thereby counteracting the tendency of RPA to overestimate band gaps. Thus, in oxides the band gaps are reduced by typically 0.3–0.6 eV relative to the RPA, which generally improves the band-gap prediction in main-group oxides. For example, the direct  $\Gamma$ - $\Gamma$  gaps of MgO, CaO, and SrO are calculated as 7.87, 7.14, and 6.03 eV in  $GW^{\text{LF}}$  with GGA wave functions, in good agreement with the experimental values of 7.83, 7.09, and 5.90 eV, respectively.<sup>80,81</sup> (The indirect  $\Gamma$ - $X$  gap of SrO is calculated at 5.45 eV, close to the experimental absorption edge at 5.30 eV.<sup>82</sup>) In the  $3d$  oxides the LF effects are, however, not sufficient to achieve acceptable agreement with experiment. For example, the gap of TiO<sub>2</sub> is reduced from 4.48 eV in  $GW^{\text{RPA}}$  to 4.06 eV in  $GW^{\text{LF}}$ , and the Cu<sub>2</sub>O gap is reduced from 1.59 to 0.93 eV. Thus, while the effect in TiO<sub>2</sub> does not go far enough, the Cu<sub>2</sub>O gap is now much too small.

The observation that the  $GW^{\text{LF}}$  approach is very accurate for main-group compounds suggests that the band-structure features due to states with  $s$ - and  $p$ -like atomic orbital character should be also accurately described in TM compounds. Then, a specific treatment of the  $d$  states via an on-site potential, similar to that in the DFT +  $U$  formalism,<sup>73,74</sup> could serve to mitigate the problems arising from the presence of  $d$  states close to the band-edge energies. Since the precise nature of the issues related to  $d$  states in  $GW$  is yet unclear, such an approach is empirical in nature and serves as a phenomenological solution. However, a technical justification for this approach derives from the fact that the on-site potential acts exclusively on the problematic  $d$  orbitals and does not affect the compatibility of the  $GW$  scheme with other  $sp$  elements, e.g., in ternary compounds containing both TM and main-group cations. Further, if a sufficient degree of transferability of the empirical parameters is given, i.e., if the same on-site term for a given TM element improves the results systematically for multiple compounds, then this approach can be expected to provide an improved reliability for band-structure predictions in transition metal compounds within a single  $GW$  scheme.

The fact that within the present  $GW^{\text{RPA}}$  baseline approach the  $d$ -orbital energies lie too high in energy for both occupied  $d$  shells (as in ZnO, Cu<sub>2</sub>O) and unoccupied  $d$  shells (as in TiO<sub>2</sub> and V<sub>2</sub>O<sub>5</sub>) suggests that the average  $d$ -orbital energy could be lowered by an attractive on-site potential for  $d$  states,  $V_d < 0$ , to be applied in addition to the  $GW$  self-energy operator. The common on-site potential of the DFT +  $U$  form<sup>73</sup> is, however, not suitable for this purpose because it creates an attractive

potential  $V_{\text{DFT}+U} < 0$  only for occupied states, but a repulsive potential  $V_{\text{DFT}+U} > 0$  for unoccupied states. Therefore, the nonlocal external potential of the form<sup>83</sup>

$$\hat{V}_{a,l} = \sum_{i,i'} |p_i\rangle \langle \phi_i | V_{a,l} | \phi_{i'} \rangle \langle p_{i'} |$$

is employed here instead, where the  $p$  and  $\phi^{\text{AE}}$  are the PAW projectors and all electron partial waves, respectively, which depend on an index  $i$  ( $i'$ ) that comprises the atomic site  $a$ , the angular-momentum numbers  $l, m$  and an index  $k$  for the reference energy<sup>39</sup> The strength of the on-site potential is defined by the parameter  $V_d$  ( $V_{a=\text{TM},l=2}$ ), which in contrast to the DFT +  $U$  potential is not occupation dependent.

For each of the TM cations, the parameter  $V_d$  has been adjusted so to reach the best agreement with the above cited experimental data from Refs. 42–71. The above described considerations regarding the determination of the band-gap energy from experiment have been taken into account, and, where available, the spectral dependence was considered for the adjustment [e.g., the energy dependence of the imaginary part of the dielectric function in case of V<sub>2</sub>O<sub>5</sub> (Ref. 47)]. Table I lists the resulting band-gap energy, the optical absorption threshold for direct-allowed transitions,<sup>84</sup> the electronic dielectric constant  $\epsilon$ , and the magnitude of  $V_d$  for the respective TM cation. Figure 1 shows the local density of states and the absorption spectrum, calculated in the independent-particle approximation (i.e., excluding excitonic effects). Note that the absorption spectra also do not include phonon-assisted or disorder-induced indirect/forbidden transitions.

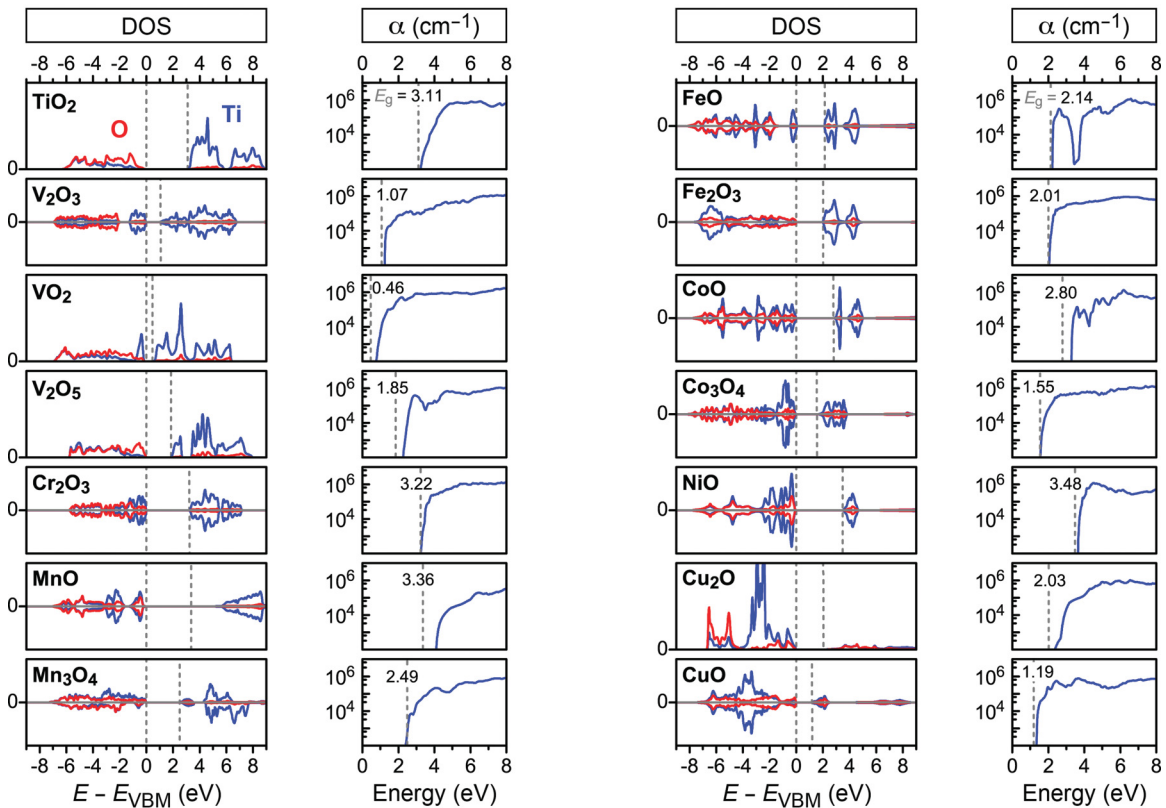


FIG. 1. (Color online) The density of states (DOS) and absorption coefficient  $\alpha$  for the  $3d$  oxides calculated in  $GW^{\text{LF}} + V_d$ . In spin-polarized cases, the spin-up and spin-down DOS are shown to positive and negative values. Dashed lines indicate the band-gap energy  $E_g$ .

It is an encouraging observation that good agreement of the band-gap energies with experiment can be achieved with a single parameter  $V_d$  per TM atom even in those cases where different oxide stoichiometries and TM oxidation states are available (Table I). Notably,  $V_d = -2.0$  eV for Fe compensates for both the underestimated gap of FeO ( $E_g = 1.31$  eV in  $GW^{LF}$  without  $V_d$ ) and the overestimated gap of  $Fe_2O_3$  ( $E_g = 3.09$  eV in  $GW^{LF}$  without  $V_d$ ). Similarly, also in case of the Cu oxides, a correction of  $E_g$  in opposite directions is achieved with a single  $V_d$  parameter (Table I). Generally, one can expect that a negative value for  $V_d$  will lead to a significant increase of  $E_g$  in compounds such as FeO or  $Cu_2O$  where the occupied TM- $d$  states lie close to the valence band maximum (VBM), but to a decrease of  $E_g$  in compounds such as  $Fe_2O_3$  or CuO where the unoccupied TM- $d$  states lie close to the conduction band minimum (CBM) (cf. Fig. 1). The observation that a single parameter  $V_d$  leads to a much improved band-gap energy in either situation strongly suggests that the difficulties encountered in standard  $GW$  calculations for TM compounds relate mostly to the *average*  $d$ -orbital energy, and not so much the exchange splitting between the majority/minority spin directions or the splitting between occupied and unoccupied  $d$  symmetries. Therefore, the appropriate magnitude of  $V_d$  should be rather insensitive on the local environment, and there is reason to believe that  $GW^{LF} + V_d$  could be suitable for predictions of a wider range of transition metal compounds that have not yet been extensively studied experimentally. For example, we recently investigated in a related study the ternary oxide  $Cr_2MnO_4$ ,<sup>85</sup> where the experimental band gap was determined to lie around 3.2–3.4 eV. While the  $GW^{RPA}$  approach largely overestimates the gap at  $E_g = 4.7$  eV, the  $GW^{LF} + V_d$  scheme yields 3.3 eV with the same parameters as determined in the present work.

## V. BAND ORDERING IN $Cu_2O$ IN DIFFERENT $GW$ SCHEMES

$Cu_2O$  is a  $p$ -type semiconductor that recently received renewed interest as a photovoltaic and photocatalytic material.<sup>3,4,29,69,86</sup> While its relatively large band gap of 2.17 eV is still suitable for a wide-gap solar absorber, the optical transition at the band-gap energy is parity forbidden,<sup>68,69</sup> leading to a weak absorption onset, which is particularly detrimental in thin-film absorbers. Thus, the correct theoretical description of the energy ordering of bands with different symmetries—giving rise to allowed and forbidden transitions—is essential to realistically describe the optical properties of  $Cu_2O$  in the context of solar energy applications.

Figure 2 shows the calculated dielectric function and the absorption spectrum for  $Cu_2O$ , based on GGA +  $U$  wave functions and  $GW^{LF} + V_d$  quasiparticle energies as described above. For the calculation of these optical spectra, excitonic effects (electron-hole interactions) are included within the time-dependent hybrid functional approximation described in Ref. 79, using a constant screening factor  $1/\epsilon$  for the electron-hole exchange. Compared to previous calculations in the independent particle approximation based on a HSE band structure,<sup>87</sup> the spectrum of the imaginary part  $\epsilon_2$  shows a considerable shift of intensity to lower energies closer to the band gap, thereby improving significantly the agreement

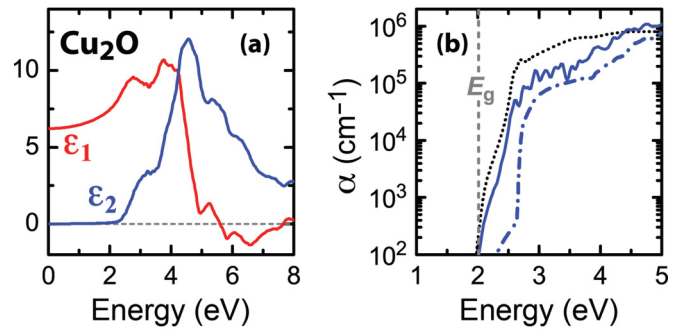


FIG. 2. (Color online) (a) The real ( $\epsilon_1$ ) and imaginary ( $\epsilon_2$ ) parts of the dielectric function and (b) the absorption coefficient ( $\alpha$ ) for  $Cu_2O$ , based on the  $GW^{LF} + V_d$  approach, including excitonic effects. For comparison, the experimental spectrum is shown as a dotted line (after Refs. 89,90), and the calculated spectrum in the independent particle approximation is shown as a dash-dotted line.

with the experimentally measured dielectric function.<sup>69,87</sup> The inclusion of excitonic effects further increases the static electronic dielectric constant from  $\epsilon = 5.7$  (Table I) to 6.2 [experiment:  $\epsilon = 6.46$  (Ref. 88)], and also leads to a near-quantitative agreement with the experimental absorption spectrum.<sup>89,90</sup> Thus, it can be concluded that the  $GW^{LF} + V_d$  approach affords a very realistic description of the band structure and optical properties of  $Cu_2O$ .

In order to facilitate a comparative evaluation of different  $GW$  schemes in regard to allowed and forbidden valence-to-conduction band transitions, the following discussion is intended to elucidate the origins of the peculiar conduction band structure of  $Cu_2O$  and its relation to the features of the cuprite structure.

Figure 3(a) shows the band structure of  $Cu_2O$  calculated in the  $GW^{LF} + V_d$  approach,<sup>91</sup> highlighting the VBM ( $\Gamma_{25'}$ ), the CBM ( $\Gamma_1$ ), and the second conduction band ( $\Gamma_{12'}$ ). Figure 3(b) shows the cuprite structure, where the unit cell is rotated so that the O-Cu-O dumbbell motif is aligned along the  $z$  axis. Due to the presence of inversion symmetry in the cuprite structure with the Cu sites as inversion center [cf. central Cu site in Fig. 3(b)], the parity of the wave functions is well defined. The  $\Gamma_{25'}$  VBM has dominantly a Cu- $d$  atomic orbital character and is of even parity. The  $\Gamma_1$  CBM has  $s$ -like contributions from both the cation and the anion, similar to other direct-gap compounds (e.g., GaAs, ZnO, MgO). However, reflecting the symmetry of the O-Cu-O dumbbell structure [Fig. 3(b)], Cu- $d_{z^2}$  and Cu- $s$  orbitals share a common point group representation ( $a_{1g}$ ), leading to an unusual intrasite  $s$ - $d$  hybridization and to a strong Cu- $d_{z^2}$  contribution to the CBM. The parity of  $\Gamma_1$  is even and, therefore, the optical transition at the band-gap energy  $E(\Gamma_1) - E(\Gamma_{25'})$  is dipole forbidden. The second conduction band ( $\Gamma_{12'}$ ) is doubly degenerate and has a Cu- $p_{xy}$  character, and it can be understood as originating from the two unoccupied atomic Cu- $4p_{xy}$  orbitals that are oriented perpendicular to the O-Cu-O dumbbell axis [cf. Fig. 3(b)]. (The respective  $4p_z$  orbital oriented along the  $z$  axis lies at much higher energies, because it has a large overlap and hybridization with the O- $p$  states of the ligands.) The  $\Gamma_{12'}$  state has odd parity; hence, the vertical  $\Gamma_{25'} \rightarrow \Gamma_{12'}$  transition is allowed, and causes the strong increase of absorption above

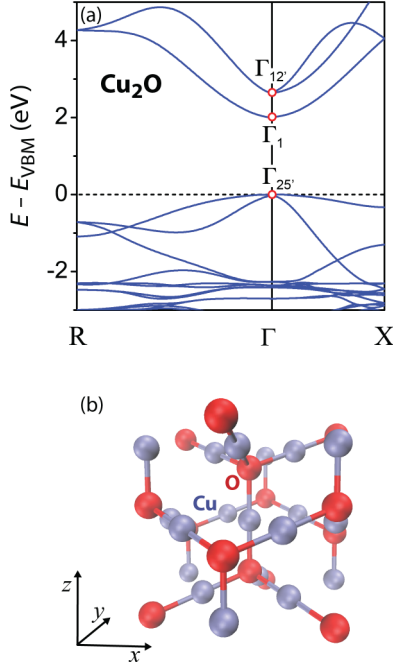


FIG. 3. (Color online) (a) The band structure of  $\text{Cu}_2\text{O}$  calculated within the  $GW^{\text{LF}} + V_d$  approach, highlighting the energies of the VBM ( $\Gamma_{25'}$ ), the CBM ( $\Gamma_1$ ), and the second conduction band ( $\Gamma_{12'}$ ) at the  $\Gamma$  point. (b) The cuprite structure, shown so as to align the O-Cu-O dumbbell motif with the  $z$  axis.

about 2.5 eV.<sup>69,90</sup> The energy difference  $\Delta E(\Gamma_{12'} - \Gamma_1) = 0.45$  eV between the first and second conduction bands has been experimentally determined from the four exciton series (yellow, green, blue, violet).<sup>68,69,92,93</sup>

Table II compares the band gaps  $E_g$ , the conduction-band energy ordering  $\Delta E(\Gamma_{12'} - \Gamma_1)$ , and the static electronic dielectric constant  $\epsilon$  in  $\text{Cu}_2\text{O}$  for a few common  $GW$  approaches besides those shown in Table I. The initial eigenenergies and wave functions are calculated either in  $GGA + U$  as above or with the HSE hybrid functional, using the conventional parameters  $\alpha = 0.25$  and  $\mu = 0.2 \text{ \AA}^{-1}$  for the fraction of Fock exchange and the range separation, respectively.<sup>34</sup> The  $GW$  QPE are calculated in the non-self-consistent single-shot “ $G_0W_0$ ,”

TABLE II. Results of different  $GW$  approaches for  $\text{Cu}_2\text{O}$  comparing the band-gap energy  $E_g$ , the energy ordering  $\Delta E(\Gamma_{12'} - \Gamma_1)$  of the first two conduction band states, and the shift  $\Delta E_{\text{VBM}}$  of the VBM energy relative to the initial Hamiltonian denoted in parentheses.

	$E_g$ (eV)	$\Delta E(\Gamma_{12'} - \Gamma_1)$	$\Delta E_{\text{VBM}}$
Experiment	2.17	+0.45	–
$GGA + U$	0.72	+1.37	–
$GW^{\text{RPA}}(GGA + U)$	1.59	–0.28	+0.68
$GW^{\text{LF}}(GGA + U)$	0.93	–0.60	+1.18
$GW^{\text{LF}} + V_d(GGA + U)$	2.03	+0.66	–0.62
HSE	2.01	+0.51	–
$G_0W_0^{\text{RPA}}(\text{HSE})$	1.91	–0.38	+0.62
$GW^{\text{RPA}}(\text{HSE})$	1.54	–0.56	+1.02
$\text{sc}GW^{\text{RPA}}$	2.38	+0.38	–

the energy self-consistent “ $GW$ ,” or the energy + wave function self-consistent “ $\text{sc}GW$ ” (Ref. 13) schemes.

The following trends are observed in Table II: The  $GGA + U$  calculation underestimates  $E_g$  and overestimates the energy difference  $\Delta E(\Gamma_{12'} - \Gamma_1)$  between the first and the second conduction band, reflecting the typical errors in local-density functionals. The quasiparticle energy calculation in  $GW^{\text{RPA}}(GGA + U)$  leads to a band gap that stays well below the experimental value, which is untypical for  $GW^{\text{RPA}}$  that is otherwise known for its small but systematic overestimation of band gaps due to an underestimated dielectric constant in RPA.<sup>11,14</sup> Also,  $GW^{\text{RPA}}$  leads to an inversion of the conduction band ordering, now incorrectly placing  $\Gamma_1$  above  $\Gamma_{12'}$ . The origin of these problems can be ascribed to a too high Cu- $d$  orbital energy, which causes an unusual upshift of the VBM ( $\Gamma_{25'}$ ) energy relative to  $GGA + U$  (Table II). Due to the above-described  $s$ - $d$  intrasite hybridization also the  $\Gamma_1$  state is strongly affected, causing the band energy inversion. (Note that the energy of the Cu- $p$  like  $\Gamma_{12'}$  state is remarkably invariant and stays within a narrow 0.2 eV interval for all Hamiltonians listed in Table II.<sup>94</sup>) The inclusion of local-field effects further aggravates these inaccuracies. The effect of the on-site potential  $V_d = -2.4$  eV in the  $GW^{\text{LF}} + V_d$  approach is to lower both the  $\Gamma_{25'}$  and  $\Gamma_1$  states which have a strong Cu- $d$  character, hence restoring the correct band ordering and band gap (cf. Table II). It should be noted that the inverted band ordering was observed before in  $G_0W_0^{\text{RPA}}(GGA)$  (Ref. 28), but not in  $G_0W_0^{\text{RPA}}(\text{LDA})$  (Refs. 24,28), indicating that the band ordering in  $GW$  can be rather sensitive on the character of the wave functions.

Turning towards the HSE hybrid functional as initial Hamiltonian, it is notable that the HSE calculation itself gives a good agreement for both  $E_g$  and the conduction band ordering, indicating a good description of the  $d$ -orbital energies [note that, in contrast, the Zn- $d$  band energy in ZnO lies significantly too high in HSE (Ref. 27)]. In the subsequent  $G_0W_0^{\text{RPA}}(\text{HSE})$  and self-consistent  $GW^{\text{RPA}}(\text{HSE})$  calculations, the band gap is reduced and the band ordering is inverted, leading to a qualitatively wrong description similar to the  $GW^{\text{RPA}}(GGA + U)$  result. Thus, the present findings contradict the conclusion of Ref. 29, that the  $G_0W_0(\text{HSE})$  approach appropriately describes the electronic structure of  $\text{Cu}_2\text{O}$ . As seen by the  $GW^{\text{RPA}}$  entries in Table II, the difference between the  $GGA + U$  and HSE wave functions has only a modest effect on the final results when the eigenenergies are iterated to self-consistency.

Finally, considering the  $\text{sc}GW^{\text{RPA}}$  approach it is observed that the self-consistency of the wave functions lowers the Cu- $d$  orbital energy, to a similar effect as the application of the  $V_d$  potential, i.e., to lower both the  $\Gamma_{25'}$  and  $\Gamma_1$  states relative to the  $\Gamma_{12'}$  state [cf. Fig. 3(a) (Ref. 94)], thereby increasing the band gap and correcting the band ordering. The slight overestimation of the band gap (cf. Table II) is as expected for the RPA, indicating that the description of  $\text{Cu}_2\text{O}$  in  $\text{sc}GW$  is consistent with that of main-group compounds. The present result is in line with previous  $\text{sc}GW$  calculations for  $\text{Cu}_2\text{O}$ .<sup>24,28</sup> It is somewhat surprising that the change of the wave functions in  $\text{sc}GW$  relative to  $GGA + U$  causes changes in  $E_g$  and  $\Delta E(\Gamma_{12'} - \Gamma_1)$  that are much larger and in opposite direction compared to the changes due to HSE

wave functions (cf. Table II). This observation implies that the effect of *scGW* on the wave functions is qualitatively different from that of the inclusion of Fock exchange in the HSE hybrid functional. The success of *scGW* for  $\text{Cu}_2\text{O}$  raises the question of how far the *scGW* approach can overcome in general the difficulties for transition metal compounds as described in Sec. III above. Note, however, that self-consistency of the wave functions did not resolve the problem of the too high  $\text{Zn-}d$  energies in  $\text{ZnO}$ .<sup>13,37</sup> Thus, a universal *ab initio GW* approach for TM compounds is not yet available, and may require addressing simultaneously a number of separate issues, such as vertex corrections and excitonic effects, the use of PAW potentials with improved scattering properties at high energies, or the treatment of deeper semicore states as valence electrons, all of which increase the computational overhead. Coming at the expense of introducing one empirical parameter per TM cation, the  $GW^{\text{LF}} + V_d$  approach seems promising for reasonably accurate and computationally feasible band-structure predictions in TM compounds.

## VI. CONCLUSIONS

The *GW* approximation has proven to be quite accurate for band-structure calculations in main-group compounds, but the consistent prediction of transition metal compounds remains problematic. A range of different “flavors” of *GW* are currently employed in the community, differing, e.g., in the type of the Hamiltonian for the calculation of the wave functions and initial single-particle energies, in the degree of self-consistency, and in the approximation used to calculate the screened Coulomb interaction. Thus, it is often possible to find a *GW* scheme that describes well a given transition metal compound, but predictions for novel materials that are not yet characterized experimentally may not be reliable. For the series of binary  $3d$  transition metal oxides, a baseline *GW* scheme was tested here, in which the GGA +  $U$  wave functions are maintained, but the eigenenergies are iterated to self-consistency, and  $W$  is calculated in the random-phase

approximation. This test revealed inconsistent results with cases of both underestimation and overestimation of band gaps compared to experiment. It remains to be seen which improvements over this baseline *GW* scheme are ultimately needed to achieve a consistent description of electronic properties across a wide range of transition metal compounds. In the absence of a single universal *ab initio GW* scheme that is proven to work reliably for a wider range of transition metal compounds, the present work made use of the observation that the average  $d$ -orbital energy is the main issue, and utilized an on-site potential for the transition metal  $d$  states to achieve agreement with experimental band gaps. This approach should allow for improved predictions for transition metal compounds. The photovoltaic semiconductor  $\text{Cu}_2\text{O}$  presents a particularly delicate case, where a wrong ordering of the conduction bands occurs in common *GW* approaches. The application of the on-site potential for  $\text{Cu-}d$  has been shown not only to give the correct band gap, but also to provide a consistent description of the band ordering, the dielectric function, and the absorption spectrum, which is a prerequisite for reliable predictions in the context of solar energy applications.

## ACKNOWLEDGMENTS

This work was supported by the US Department of Energy under Contract No. DE-AC36-08GO28308 to NREL. The general study on band-structure prediction for the series of  $3d$  oxides (results of Secs. III and IV) was supported through funds from the Office of Science, Office of Basic Energy Sciences, as part of an Energy Frontier Research Center. The more detailed study on the photovoltaic material  $\text{Cu}_2\text{O}$  (Sec. V) was supported through funds from the Office of Energy Efficiency and Renewable Energy, as part of a Next Generation Photovoltaics project within the SunShot initiative. The use of high-performance computing resources of the National Energy Research Scientific Computing Center and of NREL’s Computational Science Center are gratefully acknowledged.

<sup>1</sup>Y. Furubayashi, T. Hitosugi, Y. Yamamoto, K. Inaba, G. Kinoda, Y. Hirose, T. Shimada, and T. Hasegawa, *Appl. Phys. Lett.* **86**, 252101 (2005).

<sup>2</sup>L. Yu, S. Lany, R. Kykyneshi, V. Jieratum, R. Ravichandran, B. Pelatt, E. Altschul, H. A. S. Platt, J. F. Wager, D. A. Keszler, and A. Zunger, *Adv. Energy Mater.* **1**, 748 (2011).

<sup>3</sup>A. Mittiga, E. Salza, F. Sarto, M. Tucci, and R. Vasanthi, *Appl. Phys. Lett.* **88**, 163502 (2006).

<sup>4</sup>T. Minami, Y. Nishi, T. Miyata, and J. Nomoto, *Appl. Phys. Express* **4**, 062301 (2011).

<sup>5</sup>K. Sivula, F. Le Formal, and M. Grätzel, *ChemSusChem.* **4**, 432 (2011).

<sup>6</sup>L. Hedin, *Phys. Rev.* **139**, A796 (1965).

<sup>7</sup>M. Usuda, N. Hamada, T. Kotani, and M. van Schilfgaarde, *Phys. Rev. B* **66**, 125101 (2002).

<sup>8</sup>W. Luo, S. Ismail-Beigi, M. L. Cohen, and S. G. Louie, *Phys. Rev. B* **66**, 195215 (2002).

<sup>9</sup>S. V. Faleev, M. van Schilfgaarde, and T. Kotani, *Phys. Rev. Lett.* **93**, 126406 (2004).

<sup>10</sup>P. Rinke, A. Qteish, J. Neugebauer, C. Freysoldt, and M. Scheffler, *New J. Phys.* **7**, 126 (2005).

<sup>11</sup>M. van Schilfgaarde, T. Kotani, and S. V. Faleev, *Phys. Rev. Lett.* **96**, 226402 (2006).

<sup>12</sup>M. van Schilfgaarde, T. Kotani, and S. V. Faleev, *Phys. Rev. B* **74**, 245125 (2006).

<sup>13</sup>M. Shishkin, M. Marsman, and G. Kresse, *Phys. Rev. Lett.* **99**, 246403 (2007).

<sup>14</sup>M. Shishkin and G. Kresse, *Phys. Rev. B* **75**, 235102 (2007).

<sup>15</sup>F. Fuchs, J. Furthmüller, F. Bechstedt, M. Shishkin, and G. Kresse, *Phys. Rev. B* **76**, 115109 (2007).

<sup>16</sup>R. Gómez-Abal, X. Li, M. Scheffler, and C. Ambrosch-Draxl, *Phys. Rev. Lett.* **101**, 106404 (2008).

<sup>17</sup>A. Schleife, C. Rödl, F. Fuchs, J. Furthmüller, and F. Bechstedt, *Phys. Rev. B* **80**, 035112 (2009).

- <sup>18</sup>E. Luppi, H. C. Weissker, S. Bottaro, F. Sottile, V. Veniard, L. Reining, and G. Onida, *Phys. Rev. B* **78**, 245124 (2008).
- <sup>19</sup>M. Shishkin and G. Kresse, *Phys. Rev. B* **74**, 035101 (2006).
- <sup>20</sup>G. Kresse, M. Marsman, L. E. Hintzschke, and E. Flage-Larsen, *Phys. Rev. B* **85**, 045205 (2012).
- <sup>21</sup>B. C. Shih, Y. Xue, P. Zhang, M. L. Cohen, and S. G. Louie, *Phys. Rev. Lett.* **105**, 146401 (2010).
- <sup>22</sup>M. Stankovski, G. Antonius, D. Waroquiers, A. Miglio, H. Dixit, K. Sankaran, M. Giantomassi, X. Gonze, M. Côté, and G. M. Rignanese, *Phys. Rev. B* **84**, 241201(R) (2011).
- <sup>23</sup>F. Bruneval, F. Sottile, V. Olevano, R. Del Sole, and L. Reining, *Phys. Rev. Lett.* **94**, 186402 (2005).
- <sup>24</sup>F. Bruneval, N. Vast, L. Reining, M. Izquierdo, F. Sirotti, and N. Barrett, *Phys. Rev. Lett.* **97**, 267601 (2006).
- <sup>25</sup>A. N. Chantis, M. van Schilfgaarde, and T. Kotani, *Phys. Rev. Lett.* **96**, 086405 (2006).
- <sup>26</sup>C. Franchini, A. Sanna, M. Marsman, and G. Kresse, *Phys. Rev. B* **81**, 085213 (2010).
- <sup>27</sup>L. Y. Lim, S. Lany, Y. J. Chang, E. Rotenberg, A. Zunger, and M. F. Toney, *Phys. Rev. B* **86**, 235113 (2012).
- <sup>28</sup>F. Bruneval, Ph.D. thesis, Ecole Polytechnique, 2005.
- <sup>29</sup>L. Y. Isseroff and E. A. Carter, *Phys. Rev. B* **85**, 235142 (2012).
- <sup>30</sup>W. Kang and M. S. Hybertsen, *Phys. Rev. B* **82**, 085203 (2010).
- <sup>31</sup>P. Liao and E. A. Carter, *Phys. Chem. Chem. Phys.* **13**, 15189 (2011).
- <sup>32</sup>C. Rödl, F. Fuchs, J. Furthmüller, and F. Bechstedt, *Phys. Rev. B* **79**, 235114 (2009).
- <sup>33</sup>H. Jiang, R. I. Gomez-Abal, P. Rinke, and M. Scheffler, *Phys. Rev. B* **82**, 045108 (2010).
- <sup>34</sup>J. Heyd, G. E. Scuseria, and M. Ernzerhof, *J. Chem. Phys.* **118**, 8207 (2003); A. V. Krukau, O. A. Vydrov, A. F. Izmaylov, and G. E. Scuseria, *ibid.* **125**, 224106 (2006).
- <sup>35</sup>I. Balberg and H. L. Pinch, *J. Magn. Magn. Mater.* **7**, 12 (1978).
- <sup>36</sup>R. F. Berger, C. J. Fennie, and J. B. Neaton, *Phys. Rev. Lett.* **107**, 146804 (2011).
- <sup>37</sup>A. R. H. Preston, A. DeMasi, L. F. J. Piper, K. E. Smith, W. R. L. Lambrecht, A. Boonchun, T. Cheiwchanamangij, J. Arnemann, M. van Schilfgaarde, and B. J. Ruck, *Phys. Rev. B* **83**, 205106 (2011).
- <sup>38</sup>P. E. Blöchl, *Phys. Rev. B* **50**, 17953 (1994).
- <sup>39</sup>G. Kresse and D. Joubert, *Phys. Rev. B* **59**, 1758 (1999).
- <sup>40</sup>S. Lany and A. Zunger, *Phys. Rev. B* **78**, 235104 (2008).
- <sup>41</sup>S. Lany and A. Zunger, *Phys. Rev. B* **81**, 113201 (2010).
- <sup>42</sup>J. Pascual, J. Camassel, and H. Mathieu, *Phys. Rev. B* **18**, 5606 (1978).
- <sup>43</sup>S. W. Lovesey, K. S. Knight, and D. S. Sivia, *Phys. Rev. B* **65**, 224402 (2002).
- <sup>44</sup>V. Simic-Milosevic, N. Nilius, H. P. Rust, and H. J. Freund, *Phys. Rev. B* **77**, 125112 (2008).
- <sup>45</sup>V. Eyert, *Ann. Phys.* **11**, 650 (2002), and references therein.
- <sup>46</sup>V. Eyert and K. H. Höck, *Phys. Rev. B* **57**, 12727 (1998), and references therein.
- <sup>47</sup>V. G. Mokerov, V. L. Makarov, V. B. Tulvinskii, and A. R. Begishev, *Opt. Spectrosc.* **40**, 58 (1976).
- <sup>48</sup>T. R. McGuire, E. J. Scott, and F. F. Grannis, *Phys. Rev.* **98**, 1562 (1955).
- <sup>49</sup>C. S. Cheng, H. Gomi, and H. Sakata, *Phys. Status Solidi A* **155**, 417 (1996).
- <sup>50</sup>T. Ivanova, M. Surtchev, and K. Gesheva, *Phys. Status Solidi A* **184**, 507 (2001).
- <sup>51</sup>S. A. Chambers, J. R. Williams, M. A. Henderson, A. G. Joly, M. Varela, and S. J. Pennycook, *Surf. Sci.* **587**, L197 (2005).
- <sup>52</sup>W. L. Roth, *Rhys. Rev.* **110**, 1333 (1958).
- <sup>53</sup>T. Usani and T. Masumi, *Physica* **86-88**(B+C), 985 (1977).
- <sup>54</sup>H. H. Chou and H. Y. Fan, *Phys. Rev. B* **10**, 901 (1974).
- <sup>55</sup>G. B. Jensen and O. V. Nielsen, *J. Phys. C* **7**, 409 (1974).
- <sup>56</sup>D. P. Dubal, D. S. Dhawale, R. R. Salunkhe, S. M. Pawar, V. J. Fulari, and C. D. Lokhande, *J. Alloys Compd.* **484**, 218 (2009).
- <sup>57</sup>H. Y. Xu, S. L. Xu, X. D. Li, H. Wang, and H. Yan, *Appl. Surf. Sci.* **252**, 4091 (2006).
- <sup>58</sup>H. K. Bowen, D. Adler, and B. H. Auker, *J. Solid State Chem.* **12**, 355 (1975).
- <sup>59</sup>L. Neel, *Ann. Phys.* **3**, 137 (1948); **4**, 249 (1949).
- <sup>60</sup>C. G. Shull, W. A. Strauser, and E. O. Wollan, *Phys. Rev.* **83**, 333 (1951).
- <sup>61</sup>G. W. Pratt, Jr. and R. Coelho, *Phys. Rev.* **116**, 281 (1959).
- <sup>62</sup>W. L. Roth, *J. Phys. Chem. Solids* **25**, 1 (1964).
- <sup>63</sup>K. J. Kim and Y. R. Park, *Solid State Comm.* **127**, 25 (2003).
- <sup>64</sup>P. S. Patil and C. D. Lokhande, *Thin Solid Films* **272**, 29 (1996).
- <sup>65</sup>R. Newman and R. M. Chrenko, *Phys. Rev.* **114**, 1507 (1959).
- <sup>66</sup>G. A. Sawatzky and J. W. Allen, *Phys. Rev. Lett.* **53**, 2339 (1984).
- <sup>67</sup>Z. Zhang, Y. Zhao, and M. Zhu, *Appl. Phys. Lett.* **88**, 033101 (2006).
- <sup>68</sup>S. Nikitine, *Excitons: Optical Properties of Solids* (Plenum Press, New York, 1969).
- <sup>69</sup>B. K. Meyer, A. Polity, D. Reppin, M. Becker, P. Hering, P. J. Klar, Th. Sander, C. Reindl, J. Benz, M. Eickhoff, C. Heiliger, M. Heinemann, J. Blasing, A. Krost, S. Shokovets, C. Müller, and C. Ronning, *Phys. Status Solidi B* **249**, 1487 (2012), and references therein.
- <sup>70</sup>B. V. Karpenko, A. V. Kuznetsov, and V. V. Dyakin, *J. Phys.: Condens. Matter* **8**, 1785 (1996).
- <sup>71</sup>F. Marabelli, G. B. Parravicini, and F. Salghetti-Drioli, *Phys. Rev. B* **52**, 1433 (1995).
- <sup>72</sup>J. P. Perdew, K. Burke, and M. Ernzerhof, *Phys. Rev. Lett.* **77**, 3865 (1996).
- <sup>73</sup>V. I. Anisimov, J. Zaanen, and O. K. Andersen, *Phys. Rev. B* **44**, 943 (1991).
- <sup>74</sup>S. L. Dudarev, G. A. Botton, S. Y. Savrasov, C. J. Humphreys, and A. P. Sutton, *Phys. Rev. B* **57**, 1505 (1998).
- <sup>75</sup>V. Stevanovic, S. Lany, X. Zhang, and A. Zunger, *Phys. Rev. B* **85**, 115104 (2012).
- <sup>76</sup>A. I. Liechtenstein, V. I. Anisimov, and J. Zaanen, *Phys. Rev. B* **52**, R5467 (1995).
- <sup>77</sup>Noncollinear spin configurations, such as in  $Mn_3O_4$  (see Ref. 55) were approximated by the closest corresponding collinear configuration.
- <sup>78</sup>B. M. Weckhuysen and R. A. Schoonheydt, *Zeolites* **14**, 360 (1994).
- <sup>79</sup>J. Paier, M. Marsman, and G. Kresse, *Phys. Rev. B* **78**, 121201(R) (2008).
- <sup>80</sup>R. C. Whited, C. J. Flaten, and W. C. Walker, *Solid State Commun.* **13**, 1903 (1973).
- <sup>81</sup>A. S. Rao and R. J. Kearney, *Phys. Status Solidi B* **95**, 243 (1979).
- <sup>82</sup>B. Ulrici, W. Ulrici, and N. N. Kovalev, *Sov. Phys. Solid State* **17**, 2305 (1976).
- <sup>83</sup>S. Lany, H. Raebiger, and A. Zunger, *Phys. Rev. B* **77**, 241201(R) (2008).
- <sup>84</sup>The optical absorption threshold in Table I is determined from the calculated spectrum (cf. Fig. 1) somewhat arbitrarily at  $\alpha = 10^3 \text{ cm}^{-1}$ .



- <sup>85</sup>H. Peng, A. Zakutayev, S. Lany, T. R. Paudel, M. d’Avezac, A. Zunger, J. D. Perkins, D. S. Ginley, A. R. Nagaraja, N. H. Perry, and T. O. Mason (unpublished).
- <sup>86</sup>A. Paracchino, V. Laporte, K. Sivula, M. Grätzel, and E. Thimsen, *Nat. Mater.* **10**, 456 (2011).
- <sup>87</sup>J. W. Park, H. Jang, S. Kim, S. H. Choi, H. Lee, J. Kang, and S. H. Wei, *J. Appl. Phys.* **110**, 103503 (2011).
- <sup>88</sup>M. O’Keeffe, *J. Chem. Phys.* **39**, 1789 (1963).
- <sup>89</sup>T. Ito, T. Kawashima, H. Yamaguchi, T. Masumi, and S. Adachi, *J. Phys. Soc. Jpn.* **67**, 2125 (1998).
- <sup>90</sup>C. Malerba, F. Biccari, C. L. A. Ricardo, M. d’Incau, P. Scardi, and A. Mittiga, *Solar Energy Mater. Solar Cells* **95**, 2848 (2011).
- <sup>91</sup>To calculate the band structure and optical properties (Figs. 2 and 3), a finer  $k$  mesh of  $16 \times 16 \times 16$  was used for the six-atom primitive cell of  $\text{Cu}_2\text{O}$ . In order to keep the computational load feasible, the response functions were calculated with a reduced energy cutoff (120 eV) and  $k$  mesh ( $4 \times 4 \times 4$ ), and the number of bands was reduced to 256. Subgap features in the absorption spectrum, stemming from broadening due to the complex shift used in the Kramers-Kronig transformation, have been subtracted.
- <sup>92</sup>J. B. Grun, M. Sieskind, and S. Nikitine, *J. Phys. Chem. Solids* **19**, 189 (1961).
- <sup>93</sup>A. Dunois, J. L. Deiss, and B. Meyer, *J. Phys. (Paris)* **27**, 142 (1966).
- <sup>94</sup>In plane-wave methods, the band energies are conventionally defined with respect to the average electrostatic potential. If the wave functions, and hence, the charge density are kept constant, this reference is maintained and the eigenenergies obtained for a given Hamiltonian (e.g.,  $GW$ ) can be expressed as a shift relative to the respective energies in the initial Hamiltonian. For the present calculations, the invariance of the energy of the  $\Gamma_{12'}$  state within a 0.2 eV interval suggests that a possible “drift” of the potential reference due to differences of the wave functions between GGA +  $U$ , HSE, and sc $GW$  is small.